A study of the fluctuations of the atmospheric planetary flow patterns represented by spherical harmonics

By ERIK ELIASEN and BENNERT MACHENHAUER, *University of Copenhagen*

(Manuscript received December 11, 1964)

ABSTRACT

A procedure used for expanding the height of a pressure surface over the Northern Hemisphere in a series of spherical-harmonic components is described. The corresponding spherical-harmonic representation of the stream function is obtained by utilizing the geostrophic balance condition. From this representation mean values for the spectral distribution of the kinetic energy at the 500 mb level for January 1957 is presented.

The behaviour of the components with the largest horizontal scales is considered at the 500 mb and the 1000 mb levels during the 90 days period from 1 December 1956 to 28 February 1957. In general each of these components exhibits smaller or larger fluctuations, and it is attempted to investigate the character of the shorter periodic fluctuations by eliminating the constant and the long periodic parts of the stream field. For the components with wavenumber 1, 2, and 3, and with the most large-scale meridional variation, the 24 hours tendency fields show a more or less regular westward propagation with mean values for the velocity of propagation, corresponding to periods about 5 days. For the components with the same wavenumbers but with the second largest meridional scales we find for the daily deviations from the 15 days mean flow displacements also mainly towards the west and also with mean values for the velocity of propagation, decreasing with decreasing horizontal scale. The mean values of the velocity of propagation obtained in this way for the different components are nearly in accordance with the velocities determined by the Rossby effect, especially if this effect is reduced somewhat by a weak divergence effect.

On the basis of the spectral form of the barotropic vorticity equation the time derivatives for the expansion coefficients as well as for the amplitude and phase angle of the stream function at the 500 mb level have been computed for each day in January 1957, for some components of the zonal flow and some of the components with wavenumber 1, 2, 5, and 6. From these time derivatives 48 hours tendencies have been evaluated and compared with the corresponding observed ones. In general it is found that the agreement is better for components with moderately large scales than for components with very large scales. To some extent this may be explained by the neglect of quasi-stationary effects, and as a very simple attempt, these are represented by a constant term. Finally the contributions from the barotropic interactions between different groups of components to the change of kinetic energy of individual components are considered.

Introduction

For the study of the atmospheric motion on the planetary scale, it seems very appropriate to represent the horizontal flow patterns as a superposition of spherical-harmonic components. Problems connected with this representation have been treated by HAURWITZ and CRAIG (1952), by GILCHRIST (1957), and by ELLSAESSER (1963). In the present paper a short account of a procedure used for obtaining a representation of the non-divergent part of the large-scale horizontal motion in terms of the spherical-harmonic components of the stream function, is given, and the results from a series of actual flow patterns are discussed. It is known that the flow patterns on the largest scales in general exhibit relatively small fluctuations about a mean state (cf. ELIASEN, 1958, and DELAND, 1964), and it is the intention of the present investigation to study more closely the nature of these fluctuations, and especially to see to what extent they are determined by the dynamics of a barotropic flow.

In so far it should be most satisfactory to

consider the spherical-harmonic representation of the flow over the whole sphere, but due to the sparingness of observations at the Southern Hemisphere, a more reliable representation may be obtained by considering only the flow over the Northern Hemisphere. So, for the present, we have restricted the performed spherical-harmonic analyses to the Northern Hemisphere, using the data from the daily 1000 mb and 500 mb charts, published in "Daily Series Synoptic Weather Maps" by U.S. Weather Bureau.

1. Spherical-harmonic representation of the height field

As the basic material we have the height z of a surface of constant pressure at a definite time as function of the latitude φ and the longitude λ. Quite generally this function may be written as the series

$$z(\varphi,\lambda) = \sum_{m=0}^{\infty} \{a_m(\varphi)\cos m\lambda + b_m(\varphi)\sin m\lambda\} = \sum_{m=0}^{\infty}\sum_{n=m}^{\infty} \{a_{m,n}\cos m\lambda + b_{m,n}\sin m\lambda\} P_{m,n}(\varphi). \tag{1}$$

The first series express a usual Fourier analysis at the different latitude circles, where m means the number of waves round the earth. The second series express an expansion of z in terms of the spherical harmonics, where the functions $P_{m,n}$ denote the associated Legendre functions of the first kind, and $n-m$ indicates the number of zero points between the north pole and the south pole. This expansion is based upon the following condition of orthogonality

$$\int_{-1}^{1} P_{m,n}(\mu)\, P_{m,n'}(\mu)\, d\mu = 0, \quad n \neq n', \tag{2}$$

where $\mu = \sin\varphi$.

As we want, however, to consider the flow only for the Northern Hemisphere, we shall utilize the following more special condition of orthogonality

$$\int_{0}^{1} P_{m,n}(\mu)\, P_{m,n'}(\mu)\, d\mu = 0, \quad n+n' \text{ even and } n \neq n'. \tag{3}$$

On the basis of this relation we may use the expansion (1) for one hemisphere with the special condition that in all terms we shall have either $n-m$ even or $n-m$ odd. Among these two possibilities we have used the case $n-m$ even. If we extend the result of the analysis to the Southern Hemisphere, this will imply that the height of the isobaric surface becomes symmetrical with respect to the equator, whereas the other case would imply that the height becomes anti-symmetrical. When we use the Legendre functions normalized in the following way

$$\int_{0}^{1} \{P_{m,n}(\mu)\}^2\, d\mu = 1, \tag{4}$$

the coefficients $a_{m,n}$ and $b_{m,n}$ are determined from the functions $a_m(\mu)$ and $b_m(\mu)$, respectively, by the following integrals

$$a_{m,n} = \int_{0}^{1} a_m(\mu)\, P_{m,n}(\mu)\, d\mu, \qquad b_{m,n} = \int_{0}^{1} b_m(\mu)\, P_{m,n}(\mu)\, d\mu. \tag{5}$$

As we have the values of z only at a network of points over the hemisphere, the coefficients $a_m(\mu)$, $b_m(\mu)$, $a_{m,n}$ and $b_{m,n}$ can be evaluated from their integral formulae only by means of quadrature sums. $a_m(\mu)$ and $b_m(\mu)$ are evaluated simply by the trapezoidal rule, using 72 equally spaced values around each latitude circle chosen, in which way the coefficients for $m < 36$ will be the same as the coefficients determined by the method of least squares, regardless of the number of harmonics used to fit the function. In order to evaluate the integrals in (5), we have used the quadrature formula of Gauss

$$\int_{0}^{1} f(\mu)\, d\mu = \sum_{k=1}^{K/2} G_k^{(K)} f(\mu_k^{(K)}),$$

where K is even, $\mu_k^{(K)}$ the roots of the Legendre polynomial $P_{o,k}$ for $\mu > 0$, and $G_k^{(K)}$ the corresponding Gauss coefficients (cf. KRYLOV, 1962). Considering only even functions of μ, this quadrature formula is of the highest algebraic degree of precision, that is, it is exact for $f(\mu)$ being any polynomial of even degree smaller than or equal to $2(K-1)$. As a consequence

we have, corresponding to (3) and (4), for n and $n' \leqslant K-1$ the condition of orthonormality

$$\sum_{k=1}^{K/2} G_k^{(K)} P_{m,n}(\mu_k^{(K)}) P_{m,n'}(\mu_k^{(K)}) = \begin{cases} 0 \text{ for } n \neq n', \text{ and } n+n' \text{ even} \\ 1 \text{ for } n = n'. \end{cases} \quad (6)$$

Using the Gauss formula with $K = 36$, we then obtain that for $n \leqslant 35$ the coefficients

$$\left.\begin{aligned} a_{m,n} &= \sum_{k=1}^{18} G_k^{(36)} a_m(\mu_k^{(36)}) P_{m,n}(\mu_k^{(36)}) \\ b_{m,n} &= \sum_{k=1}^{18} G_k^{(36)} b_m(\mu_k^{(36)}) P_{m,n}(\mu_k^{(36)}) \end{aligned}\right\} \quad (7)$$

will be the same as the coefficients determined by the condition of least squares

$$\sum_{k=1}^{18} G_k^{(36)} \left\{ a_m(\mu_k^{(36)}) - \sum_{n=m}^{N} a_{m,n} P_{m,n}(\mu_k^{(36)}) \right\}^2 = \text{minimum},$$

and the analogous for $b_{m,n}$, independent of the number of harmonics used to fit the functions $a_m(\mu)$ and $b_m(\mu)$.

In order to compute $a_{m,n}$ and $b_{m,n}$ from the expressions (7), $a_m(\mu)$ and $b_m(\mu)$ as well as $P_{m,n}(\mu)$ must be determined at the latitudes corresponding to $\mu_k^{(36)}$. As it is somewhat inconvenient to read off the heights at these latitudes, we have computed first the coefficients $a_m(\mu)$ and $b_m(\mu)$ for each 5° latitude from 10° N to 85° N. At the north pole we have $a_m = 0$ and $b_m = 0$ for $m \neq 0$, and a_0 equal to the height at the pole. To the south of 10° N the values were obtained by the assumption that a_0 is constant, equal to the value at 10° N, and that a_m and b_m for $m \neq 0$ decrease linearly with φ from the values at 10° N to zero at the equator. To the north of 10° N the values at the latitudes to be used in (7) were obtained by polynomial interpolation, using the values computed at the equally spaced latitudes plus the value at the north pole and the values at 5° N and at the equator, determined by the assumptions mentioned above. In each interpolation the five nearest points were used.

The values of $P_{m,n}(\mu_k^{(36)})$ for $m \leqslant 18$ and $n - m \leqslant 20$ were obtained, using the following recurrence relations

$$P_{m,m}(\mu) = \left\{ \left(1 + \frac{1}{2m}\right)(1-\mu^2) \right\}^{\frac{1}{2}} P_{m-1,m-1}(\mu)$$

$$P_{m,n}(\mu) = \left(\frac{4n^2-1}{n^2-m^2}\right)^{\frac{1}{2}} \mu P_{m,n-1}(\mu) - \left(\frac{(2n+1)(n-m-1)(n+m-1)}{(2n-3)(n^2-m^2)}\right)^{\frac{1}{2}} P_{m,n-2}(\mu)$$

starting with the values $P_{0,0}(\mu_k^{(36)}) = 1$. Using the Danish electronic computer GIER, in which the accuracy of a real number corresponds to 29 significant binary digits, the results for $n \leqslant 35$ were checked for computational instability with the aid of relation (6). The error was found in no case to exceed 10^{-6}. As a further check the same recurrence relations were used to compute $P_{m,n}(\mu)$ at each 5° latitude from 5° N to 85° N, and the results were compared with the values stated in the tables of BELOUSOV (1962). The difference was found not to exceed 3×10^{-6}, in any case.

For the variance, σ^2, of the considered z-field we have

$$\sigma^2 = \int_0^1 \left\{ (a_0(\mu) - a_{0,0})^2 + \tfrac{1}{2} \sum_{m=1}^{35} [(a_m(\mu))^2 + (b_m(\mu))^2] + (a_{36}(\mu))^2 \right\} d\mu$$

with the integral computed by the quadrature formula of Gauss. In order to have a measure of the importance of the different components in the representation, we may consider, for varying values of M and J, the part of the variance, $\sigma^2_{M,J}$, accounted for by the components with $m \leqslant M$ and $n - m \leqslant J$, i.e.

$$\sigma^2_{M,J} = \sum_{j=2}^{J} (a_{0,j})^2 + \tfrac{1}{2} \sum_{m=1}^{M} \sum_{j=0}^{J} \{(a_{m,m+j})^2 + (b_{m,m+j})^2\}.$$

This is illustrated in Table 1, which gives values of $\sigma^2_{M,J}$ in per cent of the total variance σ^2 of the height of the 500 mb surface on January 16, 1957. The total variance for this case is 90355 m². From the table it is seen that the variance due to the component $(m,n) = (0,2)$ is accounting for as much as 79 per cent of the total variance. Further it is seen that the total zonal mean field (the components with $m = 0$) represents about 82 per cent, the waves with wavenumber 1 to 4 represent about 16 per cent,

TABLE 1

M / J	0	4	8	12	18
0	—	0.7	0.9	0.9	0.9
2	79.3	86.2	87.0	87.1	87.1
6	80.3	95.7	97.1	97.2	97.2
12	82.0	97.9	99.6	99.7	99.8
20	82.0	98.0	99.7	99.9	99.9

and all the components with wavenumber larger than 4 only 2 per cent.

As a more specific measure of the accuracy obtained by the representation, we may consider the r.m.s. values of the residuals for an increasing number of terms in the expansion (1). If we consider the residual resulting from the expansion with $m \leqslant M$ and $n - m \leqslant J$, we obtain for the same case as in Table 1, the r.m.s. values in meters given in Table 2. Instead of breaking off the expansion in the way considered above, one could also use the break off given by the condition $n \leqslant N$, for increasing values of N. Doing this, we get for the residual in the case $N = 12$ the r.m.s. value 29 m, and in the case $N = 18$ the r.m.s. value 16 m.

TABLE 2

M / J	4	8	12	18
6	63	52	51	50
8	49	31	29	29
12	43	20	16	14
20	42	16	11	7

2. The spherical-harmonic representation of the stream function and the spectral distribution of the kinetic energy

From the analysis of the z-field we want in the first place to study the characteristics of the large-scale flow patterns, which we shall represent by the non-divergent wind field, determined from the z-field by the following geostrophic balance equation

$$f\nabla^2\psi + \nabla f \cdot \nabla\psi = 10^4 \frac{g}{\Omega R^2}\nabla^2 z, \tag{8}$$

where Ω is the angular velocity of the earth, R the radius of the earth, f the Coriolis parameter, g the acceleration of gravity, and ∇ the two-dimensional spherical gradient operator. The stream function ψ is introduced as a non-dimensional quantity by the relation

$$\vec{v} = 10^{-4}\Omega R^2 \vec{k} \times \nabla\psi, \tag{9}$$

where $\vec{v}$ means the non-divergent horizontal velocity vector, and $\vec{k}$ the unit vector normal to the surface of the earth.

The stream function is expanded in the same way as the height field, i.e.

$$\psi(\varphi, \lambda) = \sum_{m=0}^{\infty}\sum_{n=m}^{\infty}\{\alpha_{m,n}\cos m\lambda + \beta_{m,n}\sin m\lambda\}P_{m,n}(\varphi). \tag{10}$$

From the balance equation it follows that when $n - m$ is even for the z-field, we must have $n - m$ odd for the stream function. This means that the stream function will vanish at the equator, and if the result of the analysis is extended to the Southern Hemisphere the motion will be symmetrical with respect to the equator. Inserting the expansions of z and ψ into the balance equation, we obtain the following relations

$$\left.\begin{aligned}
&\frac{m(m+2)(2m+1)}{2m+3}N_{m,m+1}\alpha_{m,m+1} = \frac{10^4 g}{2\Omega^2 R^2}m(m+1)N_{m,m}\alpha_{m,m}\\
&\frac{(m+1)(m+3)2}{2m+3}N_{m,m+1}\alpha_{m,m+1} + \frac{(m+2)(m+4)(2m+3)}{(2m+7)}N_{m,m+3}\alpha_{m,m+3} = \frac{10^4 g}{2\Omega^2 R^2}(m+2)(m+3)N_{m,m+2}\alpha_{m,m+2}\\
&\text{— — — — — — — — — — — —}\\
&\frac{(n+1)(n-1)(n-m)}{2n-1}N_{m,n-1}\alpha_{m,n-1} + \frac{n(n+2)(n+m+1)}{2n+3}N_{m,n+1}\alpha_{m,n+1} = \frac{10^4 g}{2\Omega^2 R^2}n(n+1)N_{m,n}\alpha_{m,n}\\
&\text{— — — — — — — — — — — —}
\end{aligned}\right\} \tag{11}$$

TABLE 3

m: n	0	1	2	3	4	5	6	7	8	9	10	11	12	13	14	15	16	17	18	Sum
39																			0.1	0.1
38																		0.1		0.1
37																	0.1		0.1	0.2
36																0.1		0.1		0.2
35															0.1		0.1		0.1	0.3
34														0.1		0.1		0.1		0.3
33													0.1		0.1		0.1		0.2	0.5
32												0.2		0.1		0.2		0.2		0.7
31											0.2		0.2		0.2		0.2		0.2	0.9
30										0.2		0.2		0.2		0.2		0.2		1.0
29									0.3		0.2		0.2		0.2		0.2		0.2	1.3
28								0.4		0.3		0.3		0.3		0.3		0.2		1.7
27							0.4		0.4		0.3		0.3		0.2		0.3		0.3	2.2
26						0.6		0.6		0.3		0.3		0.4		0.3		0.3		2.8
25					0.9		0.5		0.4		0.4		0.5		0.5		0.3		0.3	3.7
24				1.6		0.8		0.5		0.5		0.4		0.4		0.4		0.3		5.0
23			3.1		1.0		0.7		0.4		0.5		0.5		0.5		0.4		0.4	7.4
22		5.5		1.6		0.8		0.7		0.5		0.5		0.5		0.5		0.3		10.9
21	0.4		2.4		2.0		0.7		1.0		0.8		0.6		0.4		0.5		0.3	9.0
20		4.6		2.2		0.6		0.9		0.7		0.8		0.6		0.9		0.6		11.9
19	0.5		3.5		1.1		1.1		0.9		1.1		1.0		0.8		0.6		0.6	11.4
18		4.6		1.8		1.7		1.1		1.5		1.2		0.9		0.5		0.6		14.0
17	0.8		3.4		2.2		1.5		1.4		1.4		1.7		0.8		0.5			13.7
16		4.3		2.2		2.0		1.8		1.4		2.2		1.4		0.8				16.1
15	3.5		3.9		2.6		2.9		2.7		2.2		1.7		1.0					20.6
14		5.8		2.9		4.1		3.5		4.1		2.6		0.6						23.6
13	4.1		4.1		3.9		3.0		4.6		2.9		1.1							23.8
12		4.5		9.0		7.2		7.0		4.6		1.6								34.0
11	7.2		9.0		7.2		4.9		6.2		3.1									37.6
10		10.2		11.2		6.8		6.8		2.0										37.0
9	4.2		15.3		5.8		11.6		3.5											40.5
8		22.7		20.8		15.9		8.4												67.8
7	13.8		25.9		11.6		6.0													57.2
6		19.6		43.2		11.0														73.8
5	59.3		52.6		2.6															114.4
4		3.5		3.5																7.1
3	85.1		1.0																	86.1
2		1.1																		1.1
1	199.0																			199.0
Sum:	377.9	86.6	124.3	99.9	40.8	51.6	33.4	31.7	21.6	16.2	13.2	10.3	8.0	5.5	4.8	4.1	3.3	3.1	2.6	938.8

with $$N_{m,n} = \left(\frac{(2n+1)(n-m)!}{(n+m)!}\right)^{\frac{1}{2}},$$

and the analogous relations between $\beta_{m,n}$ and $b_{m,n}$. From these relations the values of the coefficients $\alpha_{m,n}$ and $\beta_{m,n}$ are determined from the coefficients $a_{m,n}$ and $b_{m,n}$, except in the case $m = 0$. In this case, namely, the first equation vanishes, and we cannot obtain the value of $\alpha_{0,1}$. In order to overcome this difficulty, we have utilized the following relation between $\alpha_{0,1}$ and the zonal mean value of the eastward velocity component, u_0, obtained from the definition of the stream function.

$$\alpha_{0,1} = -\frac{\sqrt{3}\cdot 10^4}{2\Omega R}\int_0^{\pi/2} u_0 \cos^2\varphi\, d\varphi. \qquad (12)$$

From this relation we have computed $\alpha_{0,1}$, using at the equator the value $u_0 = 0$ and to the north of the equator the geostrophic values, evaluated by finite differences over five degrees of latitude. The remaining coefficients $\alpha_{0,n}$ are then determined from the relations (11).

TABLE 4

m: n	0	1	2	3	4	5	6	7	8	9	10	11	12	Sum
25					0.0		0.1		0.0		0.0		0.0	0.2
24				0.5		0.1		0.0		0.0		0.0		0.6
23			1.2		0.0		0.1		0.0		0.0		0.0	1.6
22		3.9		0.6		0.1		0.2		0.1		0.0		5.0
21	0.1		0.6		0.2		0.0		0.1		0.0		0.0	1.1
20		2.3		0.4		0.0		0.0		0.0		0.0		3.1
19	0.2		1.4		0.3		0.0		0.1		0.0		0.1	2.3
18		2.5		0.3		0.4		0.1		0.1		0.1		3.6
17	0.2		1.5		0.3		0.1		0.0		0.0		0.1	2.4
16		1.8		0.8		0.0		0.0		0.1		0.2		3.3
15	2.3		1.5		0.5		0.5		0.0		0.0		0.0	5.1
14		3.1		0.5		0.0		0.0		0.3		0.2		4.3
13	2.8		0.6		0.2		0.1		0.5		0.1		0.1	4.3
12		1.6		3.8		0.4		1.2		0.3		0.4		7.8
11	3.4		3.0		0.6		0.1		0.5		0.5			8.1
10		5.4		4.0		0.1		0.7		0.1				10.3
9	0.0		9.2		1.0		3.3		0.3					13.8
8		16.2		3.1		2.3		1.8						23.4
7	5.8		18.0		1.2		2.2							27.3
6		13.4		36.4		1.3								51.2
5	56.2		48.0		0.2									104.4
4		0.1		2.2										2.3
3	84.6		0.4											85.0
2		0.9												0.9
1	198.6													198.6
Sum:	354.2	51.3	85.3	52.6	4.5	4.9	6.6	4.2	1.6	1.1	0.8	1.0	0.4	570.8

On the basis of the spherical-harmonic analyses of the stream function we may now, as a fundamental characteristic, consider the spectral distribution of the kinetic energy. For the mean value over the Northern Hemisphere of $\frac{1}{2}\vec{v}^2$ at a pressure level we have in consequence of the orthonormality relations (3) and (4) the following expression

$$\frac{1}{2\pi}\int_0^1\int_0^{2\pi} \tfrac{1}{2}\vec{v}^2 d\lambda d\mu = 10^{-8}\Omega^2 R^2 \sum_{m=0}^{\infty}\sum_{n=m}^{\infty} K_{m,n} \tag{13}$$

with

$$K_{m,n} = \begin{cases} \frac{1}{2}n(n+1)\,\alpha_{0,n}^2 & \text{for } m=0 \\ \frac{1}{4}n(n+1)\,(\alpha_{m,n}^2+\beta_{m,n}^2) & \text{for } m\neq 0 \end{cases} \tag{14}$$

being a measure of the part of the kinetic energy contributed from the component with indices m and n.

The mean values of $10^{-2}K_{m,n}$ at the 500 mb level for January 1957 are shown in Table 3 for $m \leqslant 18$ and $n-m \leqslant 21$. It is seen that the largest individual contributions are found for the components with the smaller values of m and n, i.e. from the components with the largest scales. So the contributions from the zonal flow, $m=0$, are together 40.3 per cent, and the contributions from the wavenumbers 1, 2 and 3 are together 33.3 per cent of the total contribution from all the components in the table. The contribution from the 16 components with $m \leqslant 3$ and $n-m \leqslant 7$ becomes as much as 61.5 per cent of the contribution from all the 209 components.

Together with the mean values for January of the spectral contributions we may consider also the spectral distribution for the mean flow of January, determined from the mean values of $\alpha_{m,n}$ and $\beta_{m,n}$. Omitting the very small values for the components with m larger than 12 and n larger than 25, the result is shown in Table 4, still for the 500 mb level. It is seen that the contributions are smaller than the mean values in Table 3, especially for the components with the larger values of m and n, i.e. for the components with the smaller scales. The total kinetic energy of the zonal components, $m=0$, in the mean flow is 93.7 per cent of the corresponding mean value. For the wavenumbers from 1 to 3

TABLE 5

	500 mb			1000 mb		
(m, n)	$\overline{A_{m,n}}$	$A^*_{m,n}$	$\delta^*_{m,n}$	$\overline{A_{m,n}}$	$A^*_{m,n}$	$\delta^*_{m,n}$
(1,2)	9.5	8.8	330	5.6	3.7	70
(1,4)	9.6	3.9	55	12.8	11.1	122
(1,6)	16.6	15.0	120	9.1	7.7	197
(1,8)	9.4	7.5	289	4.4	2.6	288
(2,3)	6.2	4.1	52	7.7	7.0	98
(2,5)	20.1	17.9	33	10.9	9.6	78
(2,7)	10.6	6.7	7	5.3	1.8	26
(2,9)	9.2	7.9	129	5.6	4.7	156
(3,4)	7.3	5.0	91	6.8	5.9	108
(3,6)	14.4	12.3	99	7.8	6.1	117
(3,8)	8.4	1.5	8	5.1	1.4	45
(3,10)	5.9	3.9	45	2.8	1.3	31
(4,5)	6.3	1.4	54	5.4	3.0	36
(4,7)	8.9	0.6	21	5.6	3.3	15
(4,9)	5.1	1.9	5	3.3	1.6	4
(4,11)	3.8	1.0	45	2.8	1.9	29

Finally, Table 5 contains the values, $\delta^*_{m,n}$, of the phase angle for the components in the 90 days mean flow. Here, as in the following, phase angles are given in degrees of longitude. By the total kinetic energy in the mean flow is 60.5 per cent of the corresponding mean value, a fact which clearly illustrates the permanent character of these waves. Finally the kinetic energy in the waves with wavenumbers from 4 to 18 becomes in the mean flow only 11.0 per cent of the corresponding mean value.

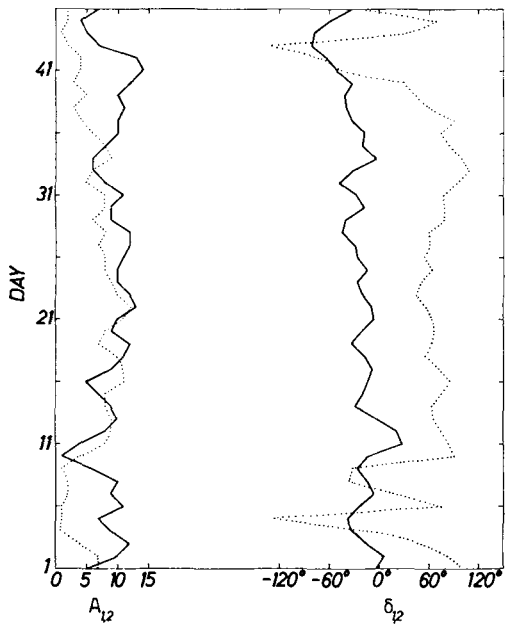

FIG. 1. Successive daily values of the amplitude (to the left) and the phase angle (to the right) for the component $(m,n) = (1,2)$ during the 45 days period, beginning 1 December 1956. Solid lines are connecting values for the 500 mb level, and dotted lines values for the 1000 mb level.

3. The fluctuations of the ultra-long waves

In this section we shall consider some results concerning the behaviour of the ultra-long waves, based on the spherical-harmonic representation of the stream function at the 500 and 1000 mb levels once a day during the 90 days period from 1 December 1956 to 28 February 1957. As we shall take into consideration only the largest scales, the work connected with the spherical-harmonic analysis has been reduced by using the height values in a rather crude network, namely the values at each 10 degrees of longitude and each 10 degrees of latitude from 10° N to 80° N. Furthermore the integrals (5) have been calculated from the values of a_m and b_m at each 10 degrees of latitude by using the trapezoidal rule.

In the decomposition (10) each component $\psi_{m,n}$ may be fixed by the amplitude $A_{m,n}$ and the phase angle $\delta_{m,n}$, i.e.

$$\psi_{m,n} = (\alpha_{m,n} \cos m\lambda + \beta_{m,n} \sin m\lambda) P_{m,n}(\varphi)$$
$$= A_{m,n} \cos \{m(\lambda - \delta_{m,n})\} P_{m,n}(\varphi).$$

Table 5 shows the mean values, $\overline{A_{m,n}}$, over the considered 90 days period of the amplitude of each of the components with wavenumbers from 1 to 4 and values of $n - m$ equal to 1, 3, 5, and 7. It is seen that the amplitude is larger at the 500 mb level than at the 1000 mb level, except for the components $(m,n) = (1,4)$ and $(2,3)$. The standard deviation of the amplitude varies for the different components between $\frac{1}{3}$ and $\frac{1}{2}$ times the mean value. Table 5, furthermore, gives the values, $A^*_{m,n}$, of the amplitude of the components in the 90 days mean flow. It is seen, that for almost all components with $m \leq 3$ the amplitude in the mean flow is only slightly smaller than the mean value of the amplitude. A marked exception is the component $(m,n) = (1,4)$, for which at the 500 mb level the amplitude in the mean flow is merely 0.4 times the mean value of the amplitude.

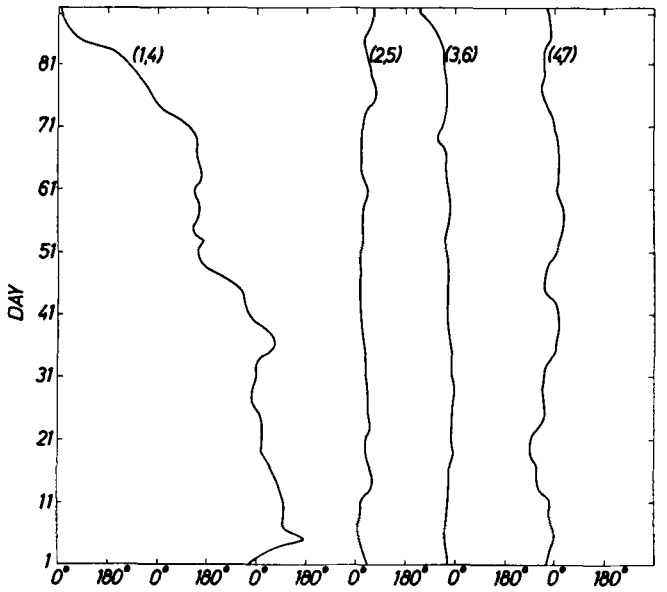

FIG. 2. Successive daily values of the phase angle at the 500 mb level for the components $(m,n) = (1,4)$, $(2,5)$, $(3,6)$, and $(4,7)$, during the 90 days period, begining 1 December 1956.

comparing the values from the two levels, it is seen that for all the components with $m \leq 3$ and $n - m \leq 5$ the position at the 500 mb level is to the west of the position at the 1000 mb level, the distance being about 0.2 times the wavelength.

The most immediate picture of the variation with time for the different components is obtained by plotting the amplitude and phase angle as function of time. For the most of the components we find relatively small fluctuations about certain mean positions, and we find rather large variations of the amplitudes. In Fig. 1 the time variation during the first half of the period is shown for the component with the largest scale, i.e. $(m,n) = (1,2)$. The amplitude is shown to the left and the phase angle to the right, with full drawn lines for the 500 mb level and dotted lines for the 1000 mb level. It is seen that most of the time the wave at the 1000 mb level is placed 50 to 100 degrees of longitude to the east of the position at the 500 mb level. The cases with the large variations in the position at the 1000 mb level are seen to occur for especially small values of the amplitude.

Fig. 2 shows the variation of the position at the 500 mb level for the components with $n - m = 3$. It is seen that for the component $(m,n) = (1,4)$ the conditions are somewhat special, in the way that this component has in two periods a steady motion towards the west, amounting in all to a displacement two times round the earth. As a consequence of this motion the amplitude of this component in the mean flow is essentially smaller than the mean value of its amplitude (Table 5). For the components $(m,n) = (2,5)$ and $(3,6)$ it is seen that the fluctuations about the mean positions are quite small. This is also the case at the 1000 mb level and the magnitude of the phase differences may be seen from the phase angles for the mean flow, given in Table 5. Concerning the component $(m,n) = (4,7)$, the figure shows that also for this component the motion must be described as fluctuations about a mean position. As, however, the fluctuations are of the same order of magnitude as the wavelength, the component is almost vanishing in the 90 days mean flow (cf. Table 5).

In order to study the character of the fluctuations of the wave components more in detail, we may consider the 24 hours changes, i.e.

$$\psi_{m,n}(t + \Delta t) - \psi_{m,n}(t)$$

where $\Delta t = 24$ hours. In this difference field the part of the motion, with periods of the

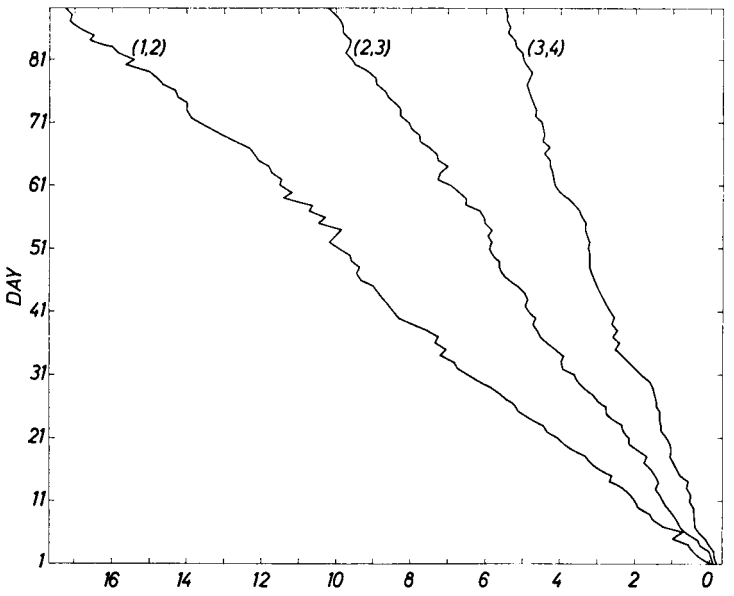

FIG. 3. Successive daily values of the phase angle for the 24 hours tendency field, $\psi_{m,n}(t+1)-\psi_{m,n}(t)$, at the 500 mb level for the components $(m,n)=(1,2)$, $(2,3)$, and $(3,4)$, during the 90 days period, beginning 1 December 1956. Abscissae are the number of westward circulations round the earth after the first passage of the Greenwich meridian.

order of or larger than 10 days will be almost eliminated. In Fig. 3 the phase angle for the 24 hours tendency field at the 500 mb level is shown as function of time for the components $(m,n)=(1,2)$, $(2,3)$, and $(3,4)$. In some few cases there has been an ambiguity by fixing the position, namely in the cases where the change from one day to the next is about half a wavelength, but for the general picture these few cases are rather insignificant. For the most large-scale component, $(m,n)=(1,2)$, it is seen that the 24 hours tendency field is moving towards the west with a rather constant speed of propagation equal to about 70 degrees of longitude per day, corresponding to a period of 5 days. For the components $(m,n)=(2,3)$ and $(3,4)$ we find a motion of the same character, with a mean speed of the westward propagation amounting to about 40 and 20 degrees of longitude per day, respectively, and the corresponding periods of 4.5 and 6 days.

If the tendency field for a wave component was moving regularly westward with a constant and sufficiently small amplitude, this would involve that the component itself should exhibit a periodic fluctuation about a mean position with a relatively large amplitude during the westward motion, and a relatively small amplitude during the eastward motion. Although the motion of the tendency field is not quite regular and its amplitude not constant, a closer inspection of the variations of the position and the amplitude of the actual wave components shows that periodic fluctuations with such a relationship between amplitude and phase velocity are found to some extent, most clearly for the component $(m,n)=(1,2)$ (cf. Fig. 1).

If we now try to consider in the same way the 24 hours tendency field for components of ultra-long waves with higher values of $n-m$, we find no distinct steady propagation, indicating that regular propagations, if any, for these components have periods essentially larger than the periods for the components considered in Fig. 3. As another method for separating the fluctuating part of a component, we may consider the field

$$\psi_{m,n}-\overline{\psi_{m,n}}^{D},$$

where the bar means a mean value over D days. By taking this difference, periods of the motion essentially larger than D days are almost

eliminated. With $D = 5$ days we obtain for the components $(m,n) = (1,2)$, $(2,3)$, and $(3,4)$ motions quite similar to those illustrated in Fig. 3. In order to investigate the fluctuations of the components with larger values of $n-m$, we may try to use larger values of D and thereby take into account larger values for the periods. Using $D = 15$ days, we obtain for the components $(m,n) = (1,4)$, $(2,5)$, and $(3,6)$ the positions of $\psi_{m,n} - \overline{\psi_{m,n}}^{D}$ at the 500 mb level shown in Fig. 4. For all three components the motion is seen to be mainly westward, with a mean speed of propagation decreasing with increasing n. For $(m,n) = (1,4)$ the mean speed is about 20 degrees of longitude per day corresponding to a period of about 18 days. For $(m,n) = (2,5)$ and $(3,6)$ the mean speed is 12 and 8 degrees of longitude per day, respectively, which is corresponding in both cases to a period of about 15 days.

Considering in the same way the fluctuations at the 1000 mb level, we find quite the same picture as at the 500 mb level, the differences in phase angle being in the mean quite small. Concerning the amplitudes, the mean values for the tendency fields considered in Fig. 3 become 2.8, 2.7, and 3.4 for $(m,n) = (1,2)$, $(2,3)$, and $(3,4)$, respectively, and for the fields considered in Fig. 4 the mean values become 4.5, 5.9, and 4.2 for $(m,n) = (1,3)$, $(2,5)$, and $(3,6)$, respectively. In general the amplitudes are somewhat smaller at the 1000 mb level than at the 500 mb level, the ratios between the mean values at the two levels being about 0.75.

The results in the foregoing may be looked upon from the following simple point of view. Writing formally

$$\psi_{m,n} = \overline{\psi_{m,n}}^{D} + (\psi_{m,n} - \overline{\psi_{m,n}}^{D}), \tag{15}$$

we have divided the component $\psi_{m,n}$ into two parts. The first part, $\overline{\psi_{m,n}}^{D}$ is to be considered as a quasi-stationary field, eventually containing fluctuations with periods essentially larger than D, and it seems reasonable to explain the existence of this quasi-stationary field primarily by the effects from the large mountain areas (CHARNEY and ELIASSEN, 1949) and the horizontal variation of heat sources (SMAGORINSKY, 1953). The second part, $\psi_{m,n} - \overline{\psi_{m,n}}^{D}$, contains the possible fluctuations with periods of the order of magnitude or smaller than D. From Fig. 3 and Fig. 4 it was seen that these fluctuations have the character of more or less regular wave propagations towards the west with a mean speed of propagation decreasing with decreasing horizontal scale. Consequently it seems natural to consider the Rossby-effect as the possible explanation of the existence of the regular moving part of the fluctuations. In order to have some quantitative information about this effect, we may consider the simple case of a barotropic, non-divergent motion of a single wave component in a zonal flow with the velocity given by

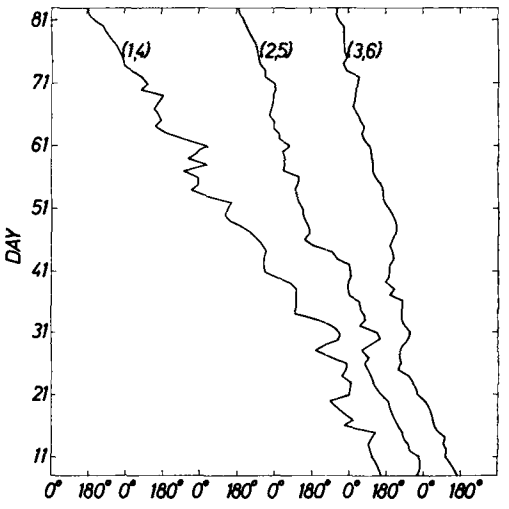

FIG. 4. Successive daily values of the phase angle for the deviation from the 15 days mean field, $\psi_{m,n} - \overline{\psi_{m,n}}^{15}$, at the 500 mb level for the components $(m,n) = (1,4)$, $(2,5)$, and $(3,6)$. The days are numbered from 1 December 1956.

$$u_0 = \omega R \cos\varphi,$$

where ω is independent of latitude. Writing the wave motion on the form

$$\psi_{m,n} = \{\alpha_{m,n} \cos m(\lambda - \gamma t) + \beta_{m,n} \sin m(\lambda - \gamma t)\} P_{m,n}(\varphi),$$

we have (HAURWITZ, 1940) the following expression for the velocity of propagation

$$\gamma = \omega - \frac{2(\omega + \Omega)}{n(n+1)}, \tag{16}$$

referred to in the following as the Rossby-Haurwitz velocity. In accordance with equation

(12), ω is determined from the coefficient $\alpha_{0,1}$ by the relation

$$\omega = -\sqrt{3} \cdot 10^{-4} \Omega \alpha_{0,1}.$$

Using for $\alpha_{0,1}$ the value -130, which is the mean value for the considered 90 days period, we get for the Rossby-Haurwitz velocity in degrees of longitude per day the values γ_{R-H}, given in the first column of Table 6. In the second column of the table we have listed the observed mean velocities of propagation, γ_{obs}, for the same components, as they are determined from Fig. 3 and Fig. 4. It is seen, that there is an essential agreement between the two sets of values, in the way that they are of the same order of magnitude, and that the values decrease rapidly with increasing values of n. Certainly the values of the Rossby-Haurwitz velocities are somewhat larger than the observed values, a fact which seems to indicate that other effects must be added as corrections.

As a simple possibility for reducing the Rossby-Haurwitz velocities, we may consider a divergence effect in the barotropic motion, as expressed by the equation

$$\frac{\partial}{\partial t}(\nabla^2 \psi) + \vec{v} \cdot \nabla \nabla^2 \psi + \frac{2\Omega}{R^2} \frac{\partial \psi}{\partial \lambda} = \frac{\varkappa}{R^2} \frac{\partial \psi}{\partial t}, \qquad (17)$$

where $\varkappa$ is treated as a constant. For the wave motion determined by this equation, the velocity of propagation will be the Rossby-Haurwitz velocity multiplied by the factor $[n(n+1)]/[\varkappa + n(n+1)]$. Using for $\varkappa$ the value 4, the values for the velocity of propagation will be reduced very close to the observed values in the last column of Table 6. It should be mentioned that this value of $\varkappa$ is essentially smaller (by a factor 0.13) than the value introduced by CRESSMAN (1958) in order to avoid the strong retrogression of the ultra-long waves in the numerical forecasting. In accordance with the formulation of the equivalent-barotropic model (cf. CHARNEY and ELIASSEN, 1949), it seems quite well possible to explain the divergence effect in the weaker form from the vertically integrated vorticity equation, by taking into account the effect of the local time derivative of the pressure at the ground with the ratio between the tendency at the ground and at the 500 mb level given by the empirical value 0.75, as stated above.

TABLE 6

(m, n)	γ_{R-H}	γ_{Obs}
(1,2)	−115	−70
(2,3)	−53	−40
(3,4) / (1,4)	−28	−20
(2,5)	−16	−12
(3,6)	− 9	− 8

4. Barotropic tendency computations

In an attempt to obtain further information about the dynamics of the fluctuations on the largest scales, we shall in the following consider a series of tendency computations on the basis of the simple equivalent-barotropic model, applied to the motion at the 500 mb level. In accordance with the expansion of the stream function in a series of orthogonal components, we shall utilize, of course, the representation of the barotropic vorticity equation in the spectral domain. For the spherical motion this representation has been formulated by SILBERMAN (1954) and discussed thoroughly in a paper by PLATZMAN (1960), in which the details behind the following brief outline may be found.

Using for (m,n) a single symbol, the expansion (10) may be written in the simplified form

$$\psi(\mu, \lambda, t) = \sum_q \chi_q(t)\, \gamma_q(\mu, \lambda),$$

where $Y_q = Y_{m,n} = P_{m,n} \cdot e^{im\lambda}$, $\chi_q = \chi_{m,n} = \frac{1}{2}(\alpha_{m,n} - i\beta_{m,n})$ for $m \neq 0$, and $\chi_{0,n} = \alpha_{0,n}$. Inserting this expansion into the non-divergent vorticity equation and multiplying by the complex conjugate of Y_p, we obtain by integrating over the sphere the following spectral form of the equation

$$\frac{1}{\Omega} \frac{d\chi_p}{dt} = \frac{2m_p}{e_p} i\chi_p + 10^{-4} \sum_{q,r} i\chi_q \chi_r S_{p,q,r} \qquad (18)$$

or

$$\left.\begin{aligned} &\frac{1}{\Omega} \frac{d\chi_p}{dt} = \frac{2 + \sqrt{3} \cdot 10^{-4}(e_p - 2)\,\alpha_{0,1}}{e_p} i m_p \chi_p + I_p, \\ &I_p = 10^{-4} \sum_{q,r} i\chi_q \chi_r S_{p,q,r}, \\ &\qquad (m_q, n_q) \text{ and } (m_r, n_r) \neq (0,1) \end{aligned}\right\} \qquad (19)$$

where $e_p = n_p(n_p+1)$, and where the interaction coefficients $S_{p,q,r}$ are determined by

$$S_{p,q,r} = \begin{cases} 0 & \text{if } m_p \neq m_q + m_r \\ \frac{1}{2}\frac{e_q - e_r}{e_p}\int_{-1}^{1} P_r\left(m_q P_q \frac{dP_r}{d\mu} - m_r P_r \frac{dP_q}{d\mu}\right) \times d\mu & \text{if } m_p = m_q + m_r. \end{cases}$$

In equation (18) the summation is taken over all combinations of q and r, but in (19) the only contribution containing $\alpha_{0,1}$ is included in the first term on the right hand side. This term, in the following referred to as the Rosby-Haurwitz term, gives the effects of the earth's rotation and the advection by the solid rotating component of the flow. The second term I_p gives the effect of the non-linear interactions between the components of the motion, apart from the solid rotation.

The time derivative of χ_p, determined by equation (19), may be resolved into the phase velocity $(d\delta_p)/(dt)$ and the amplitude tendency $(dA_p)/(dt)$. From the definitions of δ_p and A_p, we obtain by differentiation

$$\left.\begin{aligned} \frac{d\delta_p}{dt} &= (\gamma_p)_{R-H} + (\gamma_p)_I, \\ (\gamma_p)_{R-H} &= -\frac{2+\sqrt{3}\cdot 10^{-4}(e_p-2)\,\alpha_{0,1}}{e_p}\Omega, \\ (\gamma_p)_I &= -\frac{\alpha_p Im I_p + \beta_p Re I_p}{m_p A_p^2} 2\Omega \\ &= -\frac{10^{-4}\Omega}{2m_p A_p^2}\sum_{q,r}\{\alpha_p(\alpha_q\alpha_r - \beta_q\beta_r) \\ &\quad + \beta_p(\alpha_q\beta_r + \alpha_r\beta_q)\} S_{p,q,r} \end{aligned}\right\} \quad (20)$$

and

$$\left.\begin{aligned} \frac{dA_p}{dt} &= \frac{\alpha_p Re I_p - \beta_p Im I_p}{A_p} 2\Omega \\ &= \frac{10^{-4}\Omega}{2A_p}\sum_{q,r}\{\alpha_p(\alpha_q\beta_r + \alpha_r\beta_q) \\ &\quad - \beta_p(\alpha_q\alpha_r - \beta_q\beta_r)\} S_{p,q,r} \end{aligned}\right\} \quad (21)$$

where Re I_p and Im I_p represent the real and the imaginary part of I_p, respectively.

From the spherical-harmonic analyses of the stream function at the 500 mb level described in section 1 and 2, the tendencies given by (19), (20), and (21) were computed for some of the components for each day in January 1957. In these computations only the contributions from the components with $m \leq 15$ and $n - m \leq 21$ are included. As the result of the analyses indicates that the kinetic energy of the components neglected in this way is quite small, and as furthermore the components outside these boundaries must be expected to be poorly determined from the existing network of observations, it seems unlikely that an inclusion of further terms should be of any advantage. The interaction coefficients used are computed by the method described by PLATZMAN and BAER (1961), with the only difference that the Fourier coefficients of $P_{m,n}$, to be used in this method, are determined directly from the integral expressions by means of the Gauss quadrature formula. For the tendency computations to be presented in the following, the number of non-vanishing interaction coefficients is found to vary from about 300 for components with $n = 2$ and 3 to more than 900 for the component with the largest n considered, i.e. $(m,n) = (6,11)$.

In order to compare the computed barotropic tendencies with the observed changes, the mean over periods of D days of the barotropic 24-hours tendencies

$$\Delta_c(x_p) = \frac{1}{D}\int_{t_0-\frac{D}{2}\Delta t}^{t_0+\frac{D}{2}\Delta t}\left(\frac{dx_p}{dt}\right) dt, \quad \Delta t = 24 \text{ hours}$$

were evaluated by the trapezoidal rule (x_p represents any of the parameters α_p, β_p, δ_p, A_p). These mean tendencies are to be compared with the observed mean 24-hours changes, that is with the values of

$$\Delta_o(x_p) = \frac{1}{D}\left\{x_p\left(t_0 + \frac{D}{2}\Delta t\right) - x_p\left(t_0 - \frac{D}{2}\Delta t\right)\right\}.$$

Such comparisons have been made for periods up to five days. Going from $D = 1$ to $D = 2$, a better agreement was obtained for all components considered. With still higher values of D the agreement was further increased for some components but decreased for other components. In the following we shall consider only the results obtained with $D = 2$, in which case the computed mean tendency will be

$$\Delta_c(x_p) = \left\{\frac{1}{4}\left(\frac{dx_p}{dt}\right)_{t_0-\Delta t} + \frac{1}{2}\left(\frac{dx_p}{dt}\right)_{t_0} + \frac{1}{4}\left(\frac{dx_p}{dt}\right)_{t_0+\Delta t}\right\}\Delta t.$$

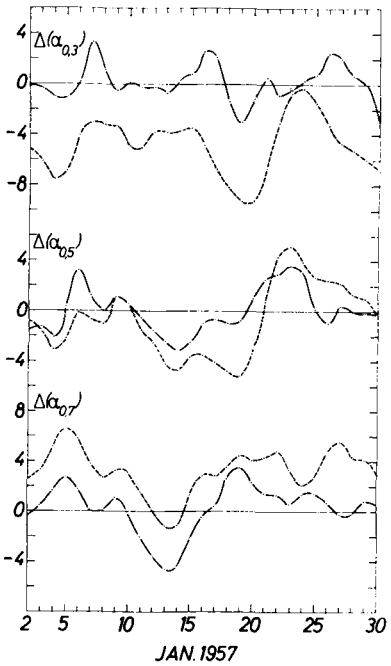

FIG. 5. Successive daily values of observed and computed tendencies of the expansion coefficient for the components $(m,n) = (0,3)$, $(0,5)$, and $(0,7)$. The solid curves show the observed values, and the dashed curves the computed values.

For the zonal mean flow the tendency computations were carried out for the components of the largest scales, $(m,n) = (0,3)$, $(0,5)$, and $(0,7)$ (the barotropic contribution to the change of the component $(m,n) = (0,1)$ is zero). In Fig. 5 the resulting values of $\Delta_o(\alpha_p)$ and $\Delta_c(\alpha_p)$ are given as function of time. The solid curves represent observed and the dashed curves computed values. The corresponding mean values, standard deviations and correlation coefficients are given in Table 7. It is seen, that for each component the observed values vary around a mean value close to zero, whereas the mean values for the computed tendencies deviate essentially from zero for the components $(m,n) = (0,3)$ and $(0,7)$. The agreement in the variation of computed and observed values is seen to increase with increasing value of n. For the component $(m,n) = (0,7)$ also a good agreement between the standard deviations for observed and computed values is found, but for the components $(m,n) = (0,3)$ and $(0,5)$ the standard deviations for the computed values are essentially larger than for the observed values. Concerning the correlation between computed and observed tendencies, the main contribution to the covariance was found to be a result of interactions between the components of the ultra-long waves with the largest meridional scales.

Among the components of the ultra-long waves the tendency computations were carried out for $(m,n) = (1,2)$, $(1,4)$, $(1,6)$, $(2,3)$, and $(2,5)$. In order to have a basis for comparison, the computations were carried out furthermore for some components of the moderately long waves, namely $(m,n) = (5,8)$, $(6,7)$, $(6,9)$, and $(6,11)$. Concerning the tendencies for the phase angle, it should be mentioned that the observed 24-hours phase changes can be determined only apart from an integer multiple of the wavelength. Generally $\Delta_o(\delta_p)$ was determined as the smallest possible displacement, but in two cases for the components $(m,n) = (2,3)$ and $(6,7)$, and in six cases for the component $(m,n) = (6,11)$ a better agreement with the computed values was obtained by using a 24-hours displacement larger than half a wavelength. When the amplitude is small, non-linear contributions to $(d\chi_p)/(dt)$ may result in large values for the computed phase velocity, and in accordance with this, the value of the amplitude was found very small in all cases with these extreme displacements. In Fig. 6 and Fig. 7 the results are illustrated for one component from each of the groups, viz. the component $(m,n) = (1,2)$ in Fig. 6*a* and *b*, and the component $(m,n) = (6,9)$ in Fig. 7. In Table 8 the mean values, the standard deviations and the correlation coefficients are stated for all the wave components considered. The correlation coefficients and the standard deviations for χ_p have been computed by using simultaneously the values of $\Delta(\alpha_p) - \overline{\Delta(\alpha_p)}$ and $\Delta(\beta_p) - \overline{\Delta(\beta_p)}$, where a bar denotes the mean value for the considered period. It is seen from the table that generally an essentially better agreement between ob-

TABLE 7

	Mean values		Stand. dev.		
(m,n)	Obs.	Comp.	Obs.	Comp.	Corr. coeff.
(0,3)	0.2	−4.8	1.4	2.2	0.44
(0,5)	0.0	−0.7	1.8	2.9	0.71
(0,7)	0.3	3.2	1.9	1.8	0.83

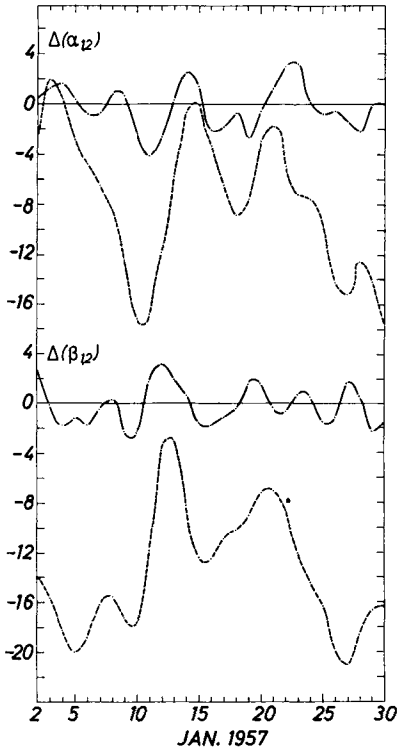

FIG. 6a. Successive daily values of observed and computed tendencies of the expansion coefficients for the component $(m,n) = (1,2)$. The solid curves show the observed values, and the dashed curves the computed values.

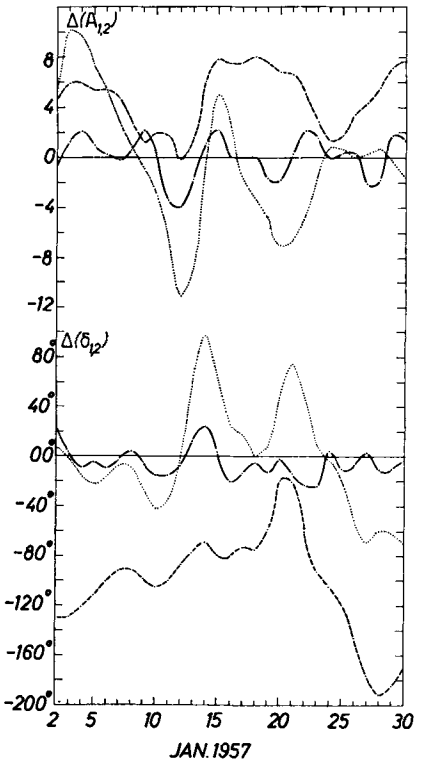

FIG. 6b. Successive daily values of observed and computed tendencies of the amplitude and the phase angle for the component $(m,n) = (1,2)$. The solid curves show the observed values, the dashed curves the values computed from the barotropic vorticity equation, and the dotted curves the values computed by including a constant term in this equation.

served and computed values is obtained for the components with $m = 5$ and 6 than for the components with $m = 1$ and 2. For the group of moderately long waves, however, it should be noted that the agreement is some what poorer for the component with the largest scale, i.e. $(m,n) = (6,7)$, than for the other components considered. Concerning the components of the ultra-long waves, we find for components with the same m a tendency to increased agreement between computed and observed values with increasing n. For the component with the smallest scale in this group, i.e. $(m,n) = (1,6)$, we find with regard to correlation coefficients and standard deviations an agreement as good as for the components with $m = 5$ and 6, whereas the differences between computed and observed mean values are somewhat larger. Concerning the correlation between computed and observed tendencies for the stream function, the covariance for the components with $n \leqslant 5$ was found to result almost exclusively from the contribution from the Rossby-Haurwitz term. As the contribution from this term to $(d\chi_p)/(dt)$, for each of these components, corresponds to an almost constant phase velocity toward the west, the large contribution to the covariance may be explained as a result of the observed fact, that the amplitude of the actual wave, in accordance with the result of the foregoing section, is relatively large, predominantly when the wave is moving towards the west, or, as for the component $(m,n) = (1,4)$, as a result of a displacement of the actual wave almost exclusively towards the west. Certainly there is also some covariance between the contributions from the non-linear terms and the observed values, but in the total computed tendencies for the components

TABLE 8

	Mean values								Standard deviations						Corr. coeff.		
	$\Delta(\alpha_{m,n})$		$\Delta(\beta_{m,n})$		$\Delta(A_{m,n})$		$\Delta(\delta_{m,n})$		$\Delta(\chi_{m,n})$		$\Delta(A_{m,n})$		$\Delta(\delta_{m,n})$		$\Delta(\chi_{m,n})$	$\Delta(A_{m,n})$	$\Delta(\delta_{m,n})$
(m, n)	Obs.	Comp.	Obs.	Comp.	Obs.	Comp.	Obs.	Comp.	Obs.	Comp.	Obs.	Comp.	Obs.	Comp.			
(1,2)	−0.1	−7.5	−0.1	−13.5	0.1	4.8	−1	−102	1.6	5.2	1.6	2.4	12	42	0.54	0.34	0.22
(2,3)	0.3	1.3	−0.1	−0.7	0.0	0.2	−14	−29	1.7	4.6	1.2	2.1	20	25	0.39	0.24	0.39
(1,4)	−0.5	−0.8	0.2	−1.5	0.1	2.1	−7	−8	1.9	3.6	1.2	2.7	17	33	0.51	0.30	0.41
(2,5)	0.6	3.5	0.2	−4.0	0.5	−0.4	0	−6	1.9	3.3	1.7	2.8	2	4	0.55	0.39	0.35
(1,6)	0.0	−0.8	0.4	2.0	0.4	2.8	0	1	2.6	3.2	2.3	2.7	16	16	0.70	0.77	0.69
(6,7)	0.1	2.2	−0.3	−0.1	−0.2	−1.9	−1	−3	1.6	2.0	1.5	2.5	12	8	0.33	0.47	0.80
(5,8)	0.4	−0.1	0.3	0.0	0.0	−0.5	3	3	2.8	2.5	2.3	2.5	8	6	0.78	0.78	0.76
(6,9)	0.3	−0.4	−0.4	−0.6	0.0	0.1	3	5	2.6	2.8	1.8	2.1	7	7	0.81	0.66	0.76
(6,11)	0.1	0.0	0.1	−0.3	0.1	0.1	11	10	2.1	2.4	1.4	2.1	20	15	0.69	0.43	0.94

with $n \leqslant 5$ the Rossby-Haurwitz contribution is dominating. For the component $(m,n) = (1,6)$ and the components of moderately long waves,

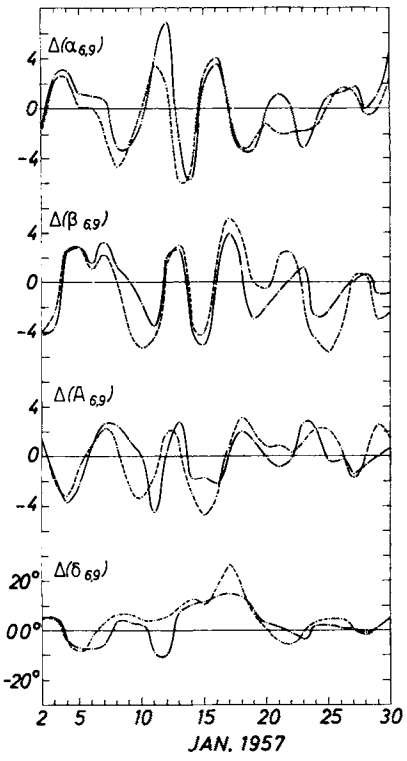

FIG. 7. Successive daily values of observed and computed tendencies of the expansion coefficients, the amplitude, and the phase angle for the component $(m,n) = (6,9)$. The solid curves show the observed values, and the dashed curves the computed values.

except $(m,n) = (6,7)$, the correlations between observed and computed tendencies are, on the other hand, determined essentially by the nonlinear terms. For the component $(m,n) = (6,7)$ the total covariance is reduced by a large negative contribution from the Rossby-Haurwitz term. Though the Rossby-Haurwitz velocity for this component amounts to a displacement towards the west of only 4 degrees of longitude per day, a displacement of the actual wave almost exclusively towards the east results in the large negative contribution. For the amplitude the contribution to the covariance from the Rossby-Haurwitz term is zero, of course, and for the phase angle the contribution is very small, simply because the Rossby-Haurwitz velocity for each component is very nearly constant.

The largest deviations between computed and observed mean values are found for the component of largest scale, i.e. $(m,n) = (1,2)$. In the mean a much too large westward phase velocity is obtained for this component. Also the components $(m,n) = (2,3)$ and, to a less extent, $(m,n) = (2,5)$ show in the mean too large westward phase velocities. The mean values of the computed phase velocities for all the considered wave components have been divided into various contributions, and the results are stated in the upper part of Table 10. The contribution from the Rossby-Haurwitz term is given in the first column. In the following columns the contribution from the nonlinear term has been divided into the contributions resulting from four groups of interactions. The group denoted W/Z includes the

TABLE 9

	Mean values		Stand. dev.		Corr. coeff.	
(m, n)	$\Delta_c(A_{m,n})$	$\Delta_c(\delta_{m,n})$	$\Delta_c(A_{m,n})$	$\Delta_c(\delta_{m,n})$	$\Delta(A_{m,n})$	$\Delta(\delta_{m,n})$
(1,2)	−0.4	− 2	5.1	43	0.55	0.53
(2,3)	0.0	−25	2.6	28	0.25	0.41
(1,4)	2.2	−10	2.6	27	0.34	0.44
(2,5)	0.3	0	3.2	4	0.56	0.53
(1,6)	0.9	− 2	2.8	19	0.73	0.63

interactions between the zonal components, except $(m,n) = (0,1)$, and the components with the same wavenumber as the considered component. The group denoted U/U includes the interactions between the components of the ultra-long waves ($m = 1$ to 4), M/M the interactions between the components with $m \geq 5$, and U/M the interactions in which one component is from the ultra-long waves and the other from the waves with $m \geq 5$. In the lower part of the table the standard deviations of the various contributions are given. Concerning the relative significance of the Rossby-Haurwitz term and the non-linear term, it is seen that only for the component with the largest scale, i.e. $(m,n) = (1,2)$, the mean contribution from the Rossby-Haurwitz term is found to be one order of magnitude larger than the mean value of the contribution from the non-linear term. For all other components the non-linear term gives an essential contribution to the total mean velocity. If daily values of $(d\delta_p)/(dt)$ are considered, it turns out that the non-linear contribution is by no means negligible. Even for $(m,n) = (1,2)$ we find that in 77 per cent of the cases the non-linear contribution amounts to more than 10 per cent of the Rossby-Haurwitz velocity, and in 19 per cent of the cases to more than 50 per cent. As to the contributions to the mean values from the various parts of the non-linear term, it is seen that for all components the interactions W/Z give relatively large positive contributions to the mean velocities, with the largest contributions for the components with the largest scales. Compared with these contributions, those resulting from the interactions U/U and especially from the interactions U/M and M/M are for most of the components small. As seen from the values of the standard deviations, the variation of the contributions from the Rossby-Haurwitz term is very small, whereas the contributions from the non-linear term have quite large fluctuations for the components with ultra-long wavelengths, except for the component $(m,n) = (2,5)$. For the interactions W/Z the standard deviations are found to be of the same magnitude as the mean values, whereas the standard deviations for the interactions U/U, U/M and M/M generally are larger than the corresponding mean values. Besides the above mentioned differences between the mean values of the computed and the observed phase velocities for the ultra-long waves, it is also seen from Table 8, that large differences between the mean values of the computed and the observed tendencies for the amplitude are found for the components with $m = 1$.

In order to account for the quasi-stationary

TABLE 10

(m, n)	R–H	W/Z	U/U	U/M	M/M	Total
		Mean values				
(1,2)	−115	17	− 7	0	2	−102
(2,3)	− 53	23	− 4	2	2	− 29
(1,4)	− 28	12	4	2	2	− 8
(2,5)	− 16	6	2	0	2	− 6
(1,6)	− 9	4	5	1	0	1
(6,7)	− 4	4	0	− 3	0	− 3
(5,8)	− 2	6	1	− 1	0	3
(6,9)	0	6	− 1	0	0	5
(6,11)	3	6	0	1	0	10
		Standard deviations				
(1,2)	1	16	24	4	11	42
(2,3)	0	28	20	5	7	25
(1,4)	0	13	15	7	17	33
(2,5)	0	2	1	1	1	4
(1,6)	0	5	13	5	6	16
(6,7)	1	3	2	6	1	8
(5,8)	1	2	3	4	3	6
(6,9)	1	2	4	6	1	7
(6,11)	0	5	3	10	3	15

TABLE 11

m: (m, n)	1	2	3	4	5	6	7	8	9	10	1–15
					Mean values						
(0,3)	1.7	−0.9	7.4	1.3	3.6	3.0	1.4	1.1	1.3	0.7	21.5
(0,5)	−1.4	2.4	−4.9	−0.2	−1.0	0.5	1.1	0.3	0.1	0.0	−2.7
(0,7)	−0.8	0.1	−2.3	−1.2	−1.9	0.0	−0.8	−0.1	−0.3	0.0	−6.9
					Standard deviations						
(0,3)	2.2	5.2	7.1	2.9	4.0	3.7	3.0	2.0	1.7	1.0	11.5
(0,5)	1.4	7.1	8.8	4.4	4.3	3.4	2.5	2.2	2.3	1.1	18.0
(0,7)	1.3	6.1	4.8	2.6	5.5	1.4	2.5	0.9	0.6	0.6	11.2

character of the ultra-long waves, we should probably include fully the effects of the inhomogeneity of the earth surface. A correct inclusion of these effects is certainly very difficult, and in the following we shall only, as a very simple possibility, consider the effects of a constant term Q_p/Ω, added to the right hand side of equation (18). The values used for Q_p are determined simply in the way that the mean values of $(d\chi_p)/(dt)$ over the considered 31 days period become zero. The only change of the results given in Table 8 for χ_p is of course a reduction of the mean values of $\Delta_c(\chi_p)$ to values almost equal to zero. For A_p and δ_p, however, changes of standard deviations and correlation coefficients as well as mean values can be expected. In Table 9 the results for A_p and δ_p, obtained by using the mentioned values of Q_p, are stated. It is seen, that an increased agreement between observed and computed values is obtained for the components $(m,n) = (1,2)$ and $(2,5)$, and it is of interest to note, that these two components are the most stationary of the components considered. For these components the differences between computed and observed mean values are reduced approximately to zero, and an improvement is also obtained for the correlation coefficients. For the component $(m,n) = (2,5)$ the standard deviations are almost unchanged, but for $(m,n) = (1,2)$ the standard deviation of $\Delta_c(A_p)$ is increased, whereas the standard deviation of $\Delta_c(\delta_p)$ is almost unchanged. For the rest of the components only small changes are obtained, apart from an improvement for the mean value of $\Delta_c(A_{1,6})$. In Fig. 6*b* the modified values of $\Delta_c(A_{1,2})$ and $\Delta_c(\delta_{1,2})$ are given as function of time by the dotted curves.

Besides the stationary effects it should be natural to consider also the divergence effect mentioned in the foregoing section, i.e. the effect of the term on the right hand side of equation (17). The inclusion of this term will imply that all tendencies are multiplied by the factor $e_p/(\varkappa + e_p)$. As a consequence the mean values and the standard deviations of the computed tendencies are reduced by this factor, whereas the correlation coefficients remain unchanged. Using for $\varkappa$ the value 4, it is seen from Table 8 and Table 9 that the differences between the standard deviations of the computed and the observed values for the components of ultra-long waves are reduced, and for most of the components this is also the case for the difference between the mean values of the observed and the computed tendencies. The standard deviations of the computed values, however, will still be larger than the standard deviations of the observed values.

For the study of the dynamics of the large-scale flow patterns the exchange of kinetic energy between the different scales must be considered as a question of fundamental importance. As a simple extension of the above tendency computations we may compute the contributions to the change of the kinetic energy of the individual components resulting from the barotropic interactions between the different components. In section 2 the quantity $K_{m,n}$ was introduced as a measure of the contribution from the component (m,n) to the total kinetic energy at a pressure level. The expression for the time rate of change of $K_{m,n}$ is determined immediately from the definition (14) of $K_{m,n}$ and the expression (21) for the time rate of change of the amplitude.

TABLE 12

(m, n)	Obs	W/Z	U/U	U/M	M/M	Total	Q	Total
				Mean values				
(1,2)	0.0	0.4	0.2	0.2	0.3	1.1	−1.2	0.0
(2,3)	0.0	−0.1	0.0	0.1	0.1	0.1	−0.1	0.0
(1,4)	0.0	0.1	0.8	0.0	0.8	1.7	0.1	1.8
(2,5)	2.0	0.3	−4.0	0.2	2.6	−0.9	3.6	2.7
(1,6)	1.2	−2.1	4.7	0.8	3.6	7.1	−5.5	1.6
(6,7)	−0.3	−4.8	0.9	0.3	0.4	−3.2		
(5,8)	0.1	−2.3	1.2	0.5	−0.6	−1.2		
(6,9)	0.4	0.5	0.2	−2.0	0.5	−0.9		
(6,11)	0.3	1.0	−0.2	−0.3	0.4	0.9		
				Standard deviations				
(1,2)	0.5	0.5	0.5	0.3	0.4	0.7	1.2	1.3
(2,3)	0.7	1.0	0.6	0.4	0.3	0.9	0.2	1.1
(1,4)	1.5	1.5	2.5	0.8	2.0	3.1	0.8	3.1
(2,5)	8.4	4.5	6.6	5.6	6.6	13.1	4.7	14.5
(1,6)	8.0	3.1	8.2	3.0	4.8	11.2	2.9	11.2
(6,7)	3.5	5.3	2.4	5.5	1.4	6.1		
(5,8)	9.8	5.5	6.7	6.9	3.6	13.0		
(6,9)	7.6	3.3	4.9	9.4	2.9	11.9		
(6 11)	5.8	4.0	3.2	4.2	2.5	7.6		

For the zonal mean flow the change of kinetic energy results entirely from the interactions between pair of components with the same wavenumber. The contributions from the different wavenumbers to the change of the kinetic energy of the components $(m,n) = (0,3)$, $(0,5)$, and $(0,7)$ are illustrated in Table 11. The numbers in the upper part of the table are the mean values of the contributions to the daily 24-hours tendencies for $10^{-2} \times K_{m,n}$, and the numbers in the lower part of the table are the corresponding standard deviations. First of all it is seen that there is a considerable transfer of kinetic energy from the wave components to the component $(m,n) = (0,3)$, whereas there is an opposite, but essentially smaller transfer for the components $(m,n) = (0,5)$ and $(0,7)$. Concerning the transfer to the component $(0,3)$, it is seen that almost all the wavenumbers contribute to it, with the largest contribution from the wavenumber 3. As the components of the zonal flow with $n > 7$ are not included in the present computations, it is not possible, of course, to make any direct comparison with the results for the conversion of the kinetic energy between the total zonal flow and the different wavenumbers, obtained by SALTZMAN and FLEISHER (1960) and by WIIN-NIELSEN, BROWN, and DRAKE (1963).

For the considered wave components the mean values and the standard deviations of the observed 24-hour changes of $10^{-2} \times K_{m,n}$ and of the contributions to the corresponding computed 24-hour tendencies are given in Table 12. Here the grouping of the non-linear interactions is the same as used in Table 10, and the numbers in the column denoted by Q are the values arising from the stationary effect introduced above. From the table it is seen that observed as well as computed changes of the kinetic energy are essentially smaller for the components $(m,n) = (1,2)$, $(2,3)$, and to a less degree $(1,4)$ than for the remaining components, which is due simply to the fact that the kinetic energy itself is relatively small for these components (cf. Table 3). For the components with wavenumber 1 the values in the table show that, in the mean, a relatively large influx of kinetic energy results from the different non-linear interactions. Further it may be noted that for all the components in the group of ultra-long waves the interactions between components with $m \geq 5$ (i.e. M/M) result, in the mean, in an influx of kinetic energy, and that for the components $(m,n) = (1,6)$, $(6,7)$, and $(5,8)$ the interactions between the zonal flow and the remaining components with the same wavenumber (i.e. W/Z) result, in the mean, in a decrease of kinetic energy.

REFERENCES

BAER, F., and PLATZMAN, G. W., 1961, A procedure for numerical integration of the spectral vorticity equation. *J. Meteor.*, **18**, pp. 393–401.

BELOUSOV, S. L., 1962, *Tables of normalized associated Legendre polynomials* (translated from the Russian). Pergamon Press, 379 pp.

CHARNEY, J. G., and ELIASSEN, A., 1949, A numerical method for predicting the perturbations of the middle latitude westerlies. *Tellus*, **1**, **2**, pp. 38–54.

CRESSMAN, G. P., 1958, Barotropic divergence and very long atmospheric waves. *Mon. Wea. Rev.*, **86**, pp. 293–297.

DELAND, R. J., 1964, Travelling planetary waves. *Tellus*, **16**, pp. 271–273.

ELIASEN, E., 1958, A study of the long atmospheric waves on the basis of zonal harmonic analysis. *Tellus*, **10**, pp. 206–215.

ELLSAESSER, H. W., 1963, Expansion of geophysical scalar fields in surface spherical harmonics. *University of Cal., LRL Rpt. UCRL-7617-T, Contr. No. W-7405-eng-48*, 48 pp.

GILCHRIST, A., 1957, The representation of circumpolar 500 mb charts by a series of spherical harmonics. *British Meteor. Off., Meteor. Res. Pap., No.* **1040**, 9 pp.

HAURWITZ, B., 1940, The motion of atmospheric disturbances on the spherical earth. *J. Marine Res.*, **3**, pp. 254–267.

HAURWITZ, B., and CRAIG, R. A., 1952, Atmospheric flow patterns and their representation by spherical surface harmonics. *U.S. Air Force, Cambr. Res. Cntr., Geophys. Res. Pap., No.* **14**, 78 pp.

KRYLOV, V. I., 1962, *Approximate calculation of integrals* (translated from the Russian). The Macmillan Company, New York, 357 pp.

PLATZMAN, G. W., 1960, The spectral form of the vorticity equation. *J. Meteor.*, **17**, pp. 635–644.

SALTZMAN, B., and FLEISHER, A., 1960, Spectrum of kinetic energy transfer due to large-scale horizontal Reynolds stresses. *Tellus*, **12**, pp. 110–111.

SILBERMAN, I., 1954, Planetary waves in the atmosphere. *J. Meteor.*, **11**, pp. 27–34.

SMAGORINSKY, J., 1953, The dynamical influence of large-scale heat sources and sinks on the quasi-stationary mean motion of the atmosphere. *Quart. J. R. Meteor. Soc.*, **79**, pp. 342–366.

WIIN-NIELSEN, A., BROWN, J. A., and DRAKE, M., 1963, On atmospheric energy conversions between the zonal flow and the eddies. *Tellus*, **15**, pp. 261–279.